Design, Synthesis, and Characterization of Templated Metal Sites in Porous Organic Hosts: Application to Reversible Dioxygen Binding

Anjal C. Sharma and A. S. Borovik*

Contribution from the Department of Chemistry, University of Kansas, Lawrence, Kansas 66045

Received April 27, 2000. Revised Manuscript Received July 12, 2000

Abstract: Porous materials with immobilized metal complexes of defined structure have wide applications in catalysis, gas storage, and sensor technology. Reported herein is the use of template copolymerization methods to design and synthesize reversible dioxygen binding sites in a porous organic host. The immobilized metal sites are formed using molecular precursors including a substitutionally inert Co(III) complex that ensures the desired square-pyramidal coordination geometry around the immobilized metal ions. Analysis of the resulting mesoporous polymer by EPR spectroscopy reveals an equilibrium of four- and five-coordinate sites which is similar to that observed for molecular analogues in solution. This equilibrium is sensitive to the solvent used to suspend the polymer, with the highest percentage of five-coordinate sites (60%) observed in CH_3NO_2, which is the same solvent used to synthesize the polymer. In the presence of dioxygen ∼90% of the immobilized sites convert to Co−O_2 adducts. Dioxygen binding to the material is reversible—revision to the dioxygen-free form is obtained by purging with N_2. The large percentage of sites involved in dioxygen binding can only occur if the spatial arrangement of ligands within the immobilized sites is maintained throughout the copolymerization process. This level of molecular control within the porous organic hosts illustrates the effectiveness of this method for developing metal complexes in solid supports.

Introduction

The design and synthesis of materials with porous networks from soluble molecular precursors has received widespread attention because of the potential for creating new materials with useful chemical or physical properties.[1] The use of discrete molecules whose properties are maintained during material formation is advantageous when their structural properties are desired in the polymer.[2] This can lead to the design of systems having defined functional properties. Recent examples of porous materials made from molecular precursors include the assembly of coordination complexes,[3] organic molecules,[4] and metallic clusters in crystalline phases,[5] as well as the mono-dispersal of inorganic[6] or organic[7] species in amorphous, highly cross-linked network polymers.

Immobilization of metal complexes into porous organic hosts by copolymerization methods is one area that has offered particular promise. Frequently in these systems, the immobilized species function as sites for the binding of external guest molecules or reactive centers for chemical transformations. Two challenges in developing these materials include access to the immobilized sites within the porous host and maintenance of the desired stereochemistry of the metal complexes in the solid state.[1] Limited accessibility to the immobilized sites often occurs because of low stability of the porous host. This is especially problematic after polymerization when chemical modifications of the material are required to induce function.

The structure of immobilized metal complexes is essential in controlling the functional properties of these materials. However, structure is often difficult to control after immobilization has taken place. The precise spatial arrangement of functional groups within an immobilized site is needed to define the primary and secondary coordination spheres around the metal centers. Difficulties arise, however, because of the inability to place key endogenous ligands in the correct locations within the immobilized sites. Spatial misplacement of these endogenous ligands within the sites usually causes dysfunction. This has been illustrated recently by Hellinga.[8] In engineered blue copper proteins, Hellinga has observed that dramatic changes in the spectral and functional properties are observed when the

(1) Yaghi, O. M.; Li, H.; Davis, C.; Richardson, D.; Groy, T. L. *Acc. Chem. Res.* **1998**, *31*, 474−484.

(2) Golden, J. H.; Deng, H.; DiSalvo, F. J.; Fréchet, J. M. J.; Thompson, P. M. *Science* **1995**, *268*, 1463−1466.

(3) (a) Fujita, M.; Kwon, Y. J.; Washizu, S.; Ogura, K. *J. Am. Chem. Soc.* **1994**, *116*, 1151−1152. (b) Gardner, G. B.; Venkataraman, D.; Moore, J. S.; Lee, S. *Nature* **1995**, *374*, 792−795. (c) Yaghi, O. M.; Li, G.; Li, H. *Nature* **1995**, *374*, 792. (d) Robson, R. In *Comprehensive Supramolecular Chemistry*; Atwood, J., Davies, J. E. D., MacNicol, D. D., Vögtle, F., Eds.; Elsevier Science: Oxford, England, 1996; Vol. 6, pp 733−755. (e) Hirsch, K. A.; Wilson, S. R.; Moore, J. S. *Inorg. Chem.* **1997**, *36*, 2960. (f) Lu, J.; Paliwala, T.; Lim, S. C.; Yu, C.; Niu, T.; Jacobson, A. J. *Inorg. Chem.* **1997**, *36*, 923−929. (g) Li, Hailian; Laine, Aaron; O'Keeffe, M.; Yaghi, O. M. *Science* **1999**, *283*, 1145−1147. (h) Eddaoudi, M.; Li, H.; Yaghi, O. M. *J. Am. Chem. Soc.* **2000**, *122*, 1391−1397.

(4) (a) MacGillivray, L. R.; Atwood, J. L. *Nature* **1997**, *389*, 469−472. (b) Russell, V. A.; Evans, C. C.; Li, W.; Ward, M. *Science* **1997**, *276*, 575−579.

(5) (a) Cayton, R. H.; Chisholm, M. H.; Huffman, J. C.; Lobkovsky, E. B. *J. Am. Chem. Soc.* **1991**, *113*, 8709−8724. (b) Hawthorne, M. F.; Zheng, G. *Acc. Chem. Res.* **1997**, *30*, 267−276.

(6) (a) Dhal, P. K.; Arnold, F. H. *Macromolecules* **1992**, *25*, 7051−7059. (b) De, B. B.; Lohray, B. B.; Sivaram, S.; Dhal, P. K. *Macromolecules* **1994**, *27*, 1291−1296. (c) Santora, B. P.; Larsen, A. O.; Gagné, M. R. *Organometallics* **1998**, *17*, 3138−3140. (d) Chen, H.; Olmstead, M. M.; Albright, R. L.; Devenyi, J.; Fish, R. H. *Angew. Chem., Int. Ed. Engl.* **1997**, *36*, 642−643. (e) Saunders, G. D.; Foxon, S. P.; Walton, P. H.; Joyce, M. J.; Port, S. N. *Chem. Commun*. **2000**, 273−274. (f) Brunkan, N. M.; Gagné, M. R. *J. Am. Chem. Soc.* **2000**, *122*, 6217−6225.

(7) (a) Wulff, G. *Angew. Chem., Int. Ed. Engl.* **1995**, *34*, 1812−1832 and references therein. (b) Mosbach, K.; Ramstrom, O. *Biotechnology* **1996**, *14*, 163−170. (c) Davis, M. E.; Katz, A.; Ahmad, W. R. *Chem. Mater.* **1996**, *8*, 1820−1839. (d) Spivak, D.; Shea, K. J. *J. Org. Chem.* **1999**, *64*, 4627−4634. (e) Haupt, K.; Mosbach, K. *Chem. Rev.* **2000**, in press.

(8) Hellinga, H. W. *J. Am. Chem. Soc.* **1998**, *120*, 10055−10066 and references therein.

10.1021/ja0014739 CCC: $19.00
Published on Web 09/02/2000

positions of key amino acid residues that bind the copper ion are altered within the immobilized active site.

To overcome these problems in porosity and stereochemical control at immobilized metal centers, we have utilized template copolymerization methods to design metal sites in highly cross-linked, porous organic hosts.[9] This copolymerization technique is modeled after those commonly used to make molecularly imprinted polymers.[6,7,10] Materials formed by this method contain channel networks that remain fixed because of the highly cross-linked organic hosts. These networks connect most of the immobilized sites to the polymer surface, thus allowing guest molecules relatively free access to the sites. We have used this method to synthesize materials containing immobilized copper and cobalt complexes: the copper polymer reversibly binds CO,[9a,b] whereas the polymer with immobilized cobalt sites reversibly binds O_2.[9c] In addition, studies on the cobalt polymers indicate that the organic hosts are able to isolate a significant number of metal sites (up to 70%) which is useful in preventing undesirable bimolecular reactions. However, these systems did not address whether the template effect that occurs during polymerization is sufficient to accurately control the stereochemistry around the metal ions.

The vast majority of materials made by template copolymerization methods have used organic-based templates. Direct examination of the immobilized site structures is difficult for organic-based templates, including determining whether the relative spatial positioning of functional groups within the immobilized sites is maintained after removal of the template.[11] Immobilization of metal complexes within porous organic hosts provides a means to address these structural issues. The diverse spectroscopic properties of metal complexes allow investigation into the site structure within organic hosts. Materials made with metal templates are most often applied to metal ion sequestration.[6d,e,7a,b,10] Recent examples have included their use in molecular recognition,[6a,f,12] catalysis,[6b,c,13] and sensing.[14] However, there are few reports on the metal complex structure within the immobilized sites and its effects on function.[6a]

As part of our program to develop new materials for the storage/release of gases, we have designed a new polymer that reversibly binds dioxygen at immobilized Co(II) centers. The success of this material as a dioxygen binder is directly correlated with the ability of the organic host to regulate the stereochemistry of the Co(II) complexes in the immobilized sites. This report describes the synthesis and characterization of this material. Spectroscopic data and dioxygen binding studies demonstrate that materials made by this copolymerization method have similar properties at the metal center compared to those observed in low molecular weight synthetic systems. Furthermore, 90% of the immobilized cobalt sites reversibly bind dioxygen at room temperature.

Experimental Section

All chemicals and solvents used were obtained from either Fisher or Aldrich unless otherwise noted. Solvents and liquid reagents used for synthesis or sample preparation were dried as follows: CH_3OH was distilled over CaH_2 under nitrogen, and 4-vinylpyridine was purified by distillation under nitrogen, and then degassed by 5 freeze−pump−thaw cycles. 4-(Dimethylamino)pyridine was purified by sublimation under vacuum, and cobalt acetate tetrahydrate was dehydrated by heating under vacuum at 120 °C for 48 h. Dioxygen was dried over molecular sieves and anhydrous $CaCl_2$. 2-Hydroxy-4-(4-vinylbenzyloxy)benzaldehyde was synthesized following literature procedures.[15]

Manipulations involving air-sensitive materials, synthesis of complexes, and preparation of polymerization samples were performed either in Schlenk-type glassware under nitrogen or in a Vacuum Atmospheres drybox operating under argon. Elemental analyses were performed either at the University of Kansas Department of Medicinal Chemistry Microlab or at Desert Analytics (Tucson, AZ). All metal analyses were performed by the Analytical Services Laboratory of the Department of Animal Sciences at Kansas State University and are presented as averages for at least three analyses.

Bis[2-hydroxy-4-(4-vinylbenzyloxy)benzaldehyde]ethylenediimine ($H_2$1).[9c] The aldehyde, 2-hydroxy-4-(4-vinylbenzyloxy)benzaldehyde (1.00 g, 3.93 mmol), was suspended in 30 mL of dry CH_3OH and stirred vigorously under N_2. Ethylenediamine (0.12 g, 2.0 mmol, 0.13 mL) was added to the reaction mixture via syringe and a bright yellow solution immediately resulted. From this bright yellow solution, a yellow solid rapidly precipitated. This mixture was allowed to stir for 4 h. The yellow solid was then isolated by filtration through a medium porosity filter frit and extracted with 30 mL of $CHCl_3$. Pure H_2**1** was obtained by slow diffusion of diethyl ether into the $CHCl_3$ extract. H_2**1** (0.97 g, 93% yield) was obtained as a bright yellow crystalline solid. ^{1}H NMR ($CDCl_3$): δ 3.84 (s, 4H, −C*H*$_2$C*H*$_2$), 5.04 (s, 4H, PhO−C*H*$_2$Ph), 5.26 (d, 2H, *cis*-H(Ph)═C*H*$_2$), 5.75 (d, 2H, *trans*-H(Ph)═C*H*$_2$), 6.46 (dd, 2H, salicyl phenyl Ar*H*), 6.49 (d, 2H, salicyl phenyl Ar*H*), 6.72 (dd, 2H, *H*(Ph)═CH$_2$), 7.09 (d, 2H, salicyl phenyl Ar*H*), 7.39 (m, 4H, styryl phenyl Ar*H*), 8.20 (s, 2H, N═C*H*), 13.62 (br s, 2H, O*H*). IR (Nujol, cm^{-1}): 3436 (OH, b), 1642 (C═N, m), 1579, 1516 (m), 1168 (s). FAB-MS (CH_3CN): *m*/*z* 533 (MH^+).

[Co^{III}1(vpy)(dmap)]PF_6. H_2**1** (0.300 g, 0.563 mmol) and *N*,*N*-(dimethylamino)pyridine (dmap) (0.0688 g, 0.563 mmol) were dissolved in 15 mL of CH_2Cl_2 under an argon atmosphere. A solution of anhydrous cobalt(II) acetate (0.0997 g, 0.563 mmol) in 5 mL of CH_3OH was added to the mixture which yielded a red-orange solution. Immediately after this color change was observed, 0.187 g (0.563 mmol) of ferricenium hexafluorophosphate dissolved in 5 mL of CH_3CN was added to the reaction mixture, yielding an intensely dark brown solution. A solution of 0.0594 g (0.563 mmol) of 4-vinylpyridine (vpy) in 5 mL of CH_2Cl_2 was then rapidly added to the above solution and allowed to stir for 1 h. The reaction mixture was concentrated under reduced pressure to yield a brown solid that was extracted with five 10 mL portions of diethyl ether to remove the ferrocene generated during oxidation. The reaction mixture was then thoroughly extracted with two 20 mL portions of $CHCl_3$. [Co^{III}**1**(vpy)(dmap)]PF_6 was obtained by vapor diffusion of cyclohexane into the $CHCl_3$ solution of the product. The dark brown microcrystalline product was isolated by filtration, washed with cyclohexane, and dried under vacuum to yield 0.42 g (0.44 mmol, 78% yield) of [Co^{III}**1**(vpy)(dmap)]PF_6. Anal. Calcd for $C_{48}H_{49}CoF_6N_5O_5P$: C, 58.84; H, 5.04; N, 7.15; Co, 6.01. Found: C, 58.83; H, 4.91; N, 7.15; Co, 5.88. ^{1}H NMR ($CDCl_3$): δ 2.93 (s, 3H, dmap C*H*$_3$), 2.95 (s, 3H, dmap C*H*$_3$), 4.09 (m with two prominent peaks, 4H, −C*H*$_2$C*H*$_2$), 5.12 (s, 4H, PhO−C*H*$_2$Ph), 5.29 (d, 2H, styryl *cis*-H(Ph)═C*H*$_2$), 5.57 (dd, 1H, pyridyl *cis*-H(Ph)═C*H*$_2$,), 5.79 (d, 2H,

(9) (a) Krebs, J. F.; Borovik, A. S. *J. Am. Chem. Soc*. **1995**, *117*, 10593−10594. (b) Krebs, J. F.; Borovik, A. S. In *Molecular and Ionic Recognition with Imprinted Polymers*; ACS Symp. Ser. No. 703; Bartsch, R. A., Maeda, M., Eds.; American Chemical Society: Washington, DC, 1998; pp 159−170. (c) Krebs, J. F.; Borovik, A. S. *Chem. Commun*. **1998**, 553−554.

(10) (a) Shea, K. J. *Trends Polym. Sci.* **1994**, *A32*, 166−172. (b) *Molecular and Ionic Recognition with Imprinted Polymers*; Bartsch, R. A., Maeda, M., Eds.; ACS Symp. Ser. No. 703; American Chemical Society: Washington, DC, 1998.

(11) Notable exceptions: (a) Shea, K. J.; Sasaki, D. Y *J. Am. Chem. Soc.* **1991**, *113*, 4109−4120. (b) Katz, A.; Davis, M. E. *Nature* **2000**, *403*, 286−289. (c) Reference 6a.

(12) (a) Fujii, Y.; Matsutani, K.; Kikuchi, K. *J. Chem. Soc., Chem. Commun.* **1985**, 415−417. (b) Arnold, F. In *Molecular and Ionic Recognition with Imprinted Polymers*; ACS Symp. Ser. No. 703; Bartsch, R. A., Maeda, M., Eds.; American Chemical Society: Washington, DC, 1998; pp 159−170.

(13) (a) De, B. B.; Lohray, B. B.; Sivaram, S.; Dhal, P. K. *Tetrahedron: Asymmetry* **1995**, *9*, 2105−2108. (b) Minutolo, F.; Pini, D.; Salvadori, P. *Tetrahedron Lett.* **1996**, *37*, 3375−3378. (c) Polburn, K.; Severin, K. *Chem. Commun.* **1999**, 2483−2484.

(14) (a) Zeng, X.; Bzhelyansky, A.; Bae, S. Y.; Jenkins, A. L.; Murray, G. M. In *Molecular and Ionic Recognition with Imprinted Polymers*; ACS Symp. Ser. No. 703; Bartsch, R. A., Maeda, M., Eds.; American Chemical Society: Washington, DC, 1998; pp 218−237. (b) Jenkins, A. L.; Uy, O. M.; Murray, G. M. *Anal. Chem.* **1999**, *71*, 373−378.

(15) Daly, J.; Witkop, B. *J. Am. Chem. Soc.* **1961**, *83*, 4787−4792.

styryl *trans*-H(Ph)═C*H*$_2$), 5.95 (dd, 1H, pyridyl trans-H(Ph)═C*H*$_2$), 6.28 (m, 4H, salicyl Ar*H*), 6.54 (m, 1H, pyridyl *H*(Ph)═CH$_2$), 6.75 (dd, 2H, styryl *H*(Ph)═CH$_2$), 6.84 (s, 2H, salicyl Ar*H*), 7.13 (m, 4H, 2 pyridyl Ar*H* and 2 dmap Ar*H*), 7.41 (m, 10H, 2 N═C*H*, and 8 styryl Ar*H*), 8.00 (m, 4 H, 2 pyridyl Ar*H* and 2 dmap Ar*H*) (all assignments were confirmed by COSY). UV−vis ($CHCl_3$, λ_{max}, nm (ϵ, $M^{-1}\cdot cm^{-1}$)): 257 (sh, 87420), 268 (104560), 316 (sh, 20570), 380 (12930), 459 (br sh, 2020). Diffuse reflectance UV−vis (1% in KBr, λ_{max}, nm): 264, 372, 470 (sh), 521. Diffuse reflectance FTIR (1% in KBr, cm^{-1}): 1624 (sh), 1615 (sh), 1606, 1542 (sh), 1527, 1144, 1126, 845 (br s, PF_6^-).

P-1·py[Co^{III}(dmap)]. Under an argon atmosphere, 0.300 g (0.312 mmol) of [Co^{III}**1**(vpy)(dmap)]PF_6, 1.162 g (5.864 mmol, 1.106 mL) of ethylene glycol dimethacrylate (EGDMA), and 0.0103 g (0.00624 mmol) of azobisisobutyronitrile (AIBN) were dissolved in 3.32 mL of CH_3NO_2. This mixture was transferred to a thick-walled pressure tube, which was tightly sealed with a Teflon screwcap. The reaction mixture was heated at 60 °C for 24 h, at which point a highly cross-linked polymer had formed in the tube. The CH_3NO_2 was removed under vacuum. The deep red insoluble P-**1·py**[Co^{III}(dmap)] polymer was ground manually using a mortar and pestle. The resultant red-brown powder was subjected to continuous Soxhlet extraction with CH_3OH for 24 h. The CH_3OH wash was analyzed for vpy and dmap content, using GC-MS: there was no evidence of removal of these compounds. This polymer was dried under vacuum and sieved to a particle size <125 μm to obtain 1.35 g (92% yield) of P-**1·py**[Co^{III}(dmap)]. Anal. Calcd for P-**1·py**[Co^{III}(dmap)]: Co, 180 μmol/g; N, 1027 μmol/g. Found: Co, 180 μmol/g; N, 1057 μmol/g. Diffuse reflectance UV−vis (20% in KBr, λ_{max}, nm): 208 (s), 268 (s), 377 (m), 480 (br sh). Diffuse reflectance FTIR (20% in KBr, cm^{-1}): 1630 (sh), 1623 (sh) 1609, 1533 (sh), 1526, 847 (intense, PF_6^-). Average surface area (BET): 230 m^2/g. Average pore diameter: 22 Å.

P-1·py[Co^{II}(dmap)]. P-**1·py**[Co^{III}(dmap)] (0.300 g, 180 μmol of Co/g of polymer) was treated with 10 mL of a saturated CH_3OH solution of $Na_2S_2O_4$. The mixture was stirred for 2 h, and the polymer was separated by filtration through a medium porosity filter frit. The resultant polymer was washed with CH_3OH and diethyl ether and dried under vacuum to obtain the reduced polymer P-**1·py**[Co^{II}(dmap)]. The filtrate and washings were analyzed for vpy and dmap content using GC-MS. This polymer was then subjected to continuous extraction with CH_3OH under N_2 and dried under an inert atmosphere. A 0.2990 g yield of brown-orange P-**1·py**[Co^{II}(dmap)] was obtained. The concentration of reduced sites was 160 μmol of Co(II)/g of polymer as determined by EPR spectroscopy.

P-1·py. Under an argon atmosphere, a suspension of 0.2500 g of P-**1·py**[Co^{II}(dmap)] in a 10 mL of 0.02 M $(NMe_4)_2$EDTA methanol solution was stirred for 24 h. The polymer was filtered through a medium porosity filter frit and washed with CH_3OH and ether. The combined filtrate and washings were analyzed for dmap content using GC-MS. The resulting yellowish brown apo polymer, P-**1·py**, was washed thoroughly with CH_3OH and diethyl ether and dried under vacuum. This method gave 0.240 g of the apo polymer, P-**1·py**. Anal. Calcd for P-**1·py**: Co, 0 μmol/g; N, 654 μmol/g. Found: Co, 28 μmol/g; N, 678 μmol/g. Diffuse reflectance FTIR (20% in KBr, cm^{-1}): 1625 (sh), 1609, 1523, 848 (w, residual PF_6^-). Diffuse reflectance UV−vis (20% in KBr, λ_{max}, nm): 223 (s), 265 (s), 382 (sh), 483 (br sh). Average surface area: 240 m^2/g. Average pore diameter: 22 Å.

P-1·py[Co^{II}]. The apo polymer, P-**1·py** (0.200 g), was suspended in 10 mL of a 0.02 M $Co(OAc)_2$ methanol solution under an argon atmosphere. This mixture was stirred for 8 h and the dark orange-brown solid, P-**1·py**[Co^{II}], was filtered through a medium porosity frit and purified by continuous extraction with CH_3OH under nitrogen for 24 h. After drying under vacuum 0.2004 g of P-**1·py**[Co^{II}] was isolated. Anal. Calcd for P-**1·py**[Co^{II}]: Co, 180 μmol/g; N, 654 μmol/g. Found: Co, 171 μmol/g; N, 621 μmol/g. Diffuse reflectance UV−vis (15% in KBr, λ_{max} nm): 221 (sh), 268 (s), 379 (sh), 472 (br, sh), 633 (w br sh). Diffuse reflectance FTIR (15% in KBr, cm^{-1}): 1653 (w), 1635 (sh), 1606, 1539 (w), 1521, 1506 (w), 848 (w, residual PF_6^-). Average surface area (BET): 270 m^2/g. Average pore diameter: 22 Å.

Poly(EGDMA) was prepared by a similar procedure to that used for making P-**1·py**[Co^{III}(dmap)] except that the template complex was omitted during polymerization. Diffuse reflectance FTIR (15% in KBr, cm^{-1}): 2980 (sh), 2952, 2887 (sh), 1730, 1475 (sh), 1453, 1255, 1162, 956, 880, 754. Average surface area (BET): 310 m^2/g. Average pore diameter: 21 Å.

Preparation of Polymer Samples for EPR Spectroscopy. All samples were prepared under argon atmosphere. Typically 15−25 mg of the samples were used. In all cases, the polymer samples were measured directly into the EPR tube. Approximately 0.5 mL of the solvent was added to the EPR tube to suspend the polymer and the tube was capped with a rubber septum.

Reversible Oxygen Binding to P-1·py[Co^{II}]. Dioxygen was purged through the EPR sample tube containing P-**1·py**[Co^{II}] for 2 min at room temperature and frozen in liquid N_2. An X-band EPR spectrum of this sample was collected at 77 K and a characteristic Co-superoxo signal was observed indicating the formation of P-**1·py**[Co−O_2]. Dinitrogen gas was then purged through the EPR tube for 3 min and an EPR spectrum collected at 77 K. The spectrum was characteristic of Co(II) sites indicating that P-**1·py**[Co^{II}] was reformed. Spin density quantification shows that this signal corresponds to 90% of the total Co content in the polymer. P-**1·py**[Co−O_2] can be regenerated by purging the EPR sample tube containing P-**1·py**[Co^{II}] for 2 min with O_2. Determination of the spin concentration of this regenerated P-**1·py**[Co−O_2] indicates that 86% of the total Co content in the polymer contributes to the signal.

Preparation of EPR Spin Quantification Standard. Cupric acetylacetonate (0.0153 g, 0.0585 mmol) and 0.0870 g of host-only polymer (polymethacrylate) were ground down in a Wig-L-Bug for 3 min. The sample container was then immersed in liquid nitrogen for 30 s, followed by further homogenization in the Wig-L-Bug for 3 min. This grind/freeze/grind cycle was repeated two times. The light blue powder (0.1020 g) obtained was 15 wt % Cu(acac)$_2$ dispersion in the polymer. Anal. Calcd: Cu, 571 μmol/g. Found: Cu, 565 μmol/g.

Determination of Swelling Ratio. These measurements were made for P-**1·py**[Co^{II}] in the solvents CH_3NO_2, $CH_3CH(NO_2)CH_3$, $C_6H_5NO_2$, diethyl ether, and cyclohexane. A 1.7 mL microcentrifuge tube was charged with 40−50 mg of appropriate polymer and 1.5 mL of solvent. The tube was capped and agitated thoroughly to ensure proper mixing. After 24 h, the sample was centrifuged for 6 min. The polymer formed a well-packed bed at the bottom of the tube and the supernatant was decanted off. The solvent swollen polymer was weighed and the swelling ratio (mass of solvent swollen polymer/mass of dry polymer) was determined. P-**1·py**[Co^{II}]: 8.3 (CH_3NO_2); 6.9 ($CH_3CH(NO_2)CH_3$); 8.1 ($C_6H_5NO_2$); 5.7 (diethyl ether); 4.3 (cyclohexane).

Physical Methods. NMR spectra were recorded on either a Varian UNITYplus-400 MHz spectrometer equipped with a Sun workstation or a Bruker DRX400 instrument equipped with an SGI INDY workstation. Mass spectra were collected on a VG analytical limited VG-ZAB FAB-MS instrument. FTIR spectra were collected either on a Mattson Sirius 100 (with the 4326 upgrade) FTIR instrument or on a Mattson Genesis series FTIR instrument. UV−vis spectra were collected on a SLM Aminco 3000 diode array spectrophotometer using 1.000 cm Supracil quartz cuvettes. Diffuse reflectance samples for [Co^{III}**1**(4-vpy)(dmap)]PF_6 were prepared by mechanically grinding a 1% w/w mixture of the complex in KBr for 3 min, followed by freezing the sample in liquid nitrogen for 30 s. The grind/freeze cycle was repeated three times. Polymer samples for diffuse reflectance spectroscopy were prepared as above except the polymer mixtures were 25% w/w in KBr. UV−vis diffuse reflectance spectra were collected on a SLM-Aminco 3000 diode array spectrophotometer using a Harrick Scientific diffuse reflectance accessory (DRA-4). FTIR diffuse reflectance spectra were collected using a Mattson Genesis series FTIR instrument interfaced with an external bench, housing a Harrick Scientific diffuse reflectance accessory (DRA-PMI) with a liquid nitrogen cooled MCT narrow band detector. The spectra were collected in single beam form using 4 cm^{-1} resolution, 512 scans, and a gain of 1. The spectra were then converted to Kubelka−Munk units using KBr as the reference material.

Quantitative analysis for dmap and vpy was performed by GC-MS using the method of internal standards, with mesitylene as the standard. GC-MS analysis was performed using a HP 6890 chromatograph coupled to a mass selective detector. Scanning electron micrographs were collected on a Hitachi S-570 SEM equipped with a LaB_6 filament.

SEM samples were prepared by coating a clean Cambridge sample with carbon graphite paint. The polymer, which was sieved to particle sizes of 250−500 μm, was then sprinkled onto the paint, and the excess polymer was shaken off. The sample stub was dried gently in an oven at 65 °C. It was then sputter coated with a 10 nm thick Au−Pd (60:40) alloy coat by using a Hummer-2 operating at 130 Torr and 10 μAmps. Samples were scanned using an accelerating voltage of 3.0 kV. Surface area analyses of the polymers were performed on a Gemini surface area microanalyzer operating at 77 K. Typical sample sizes ranged from 0.12 to 0.16 g, with polymer particle sizes of 75−125 μm.

EPR spectra were collected using a Bruker ESP-300E instrument using a TE_{102} cavity or a Bruker EMX spectrometer equipped with an ER4102ST cavity. Both instruments were previously calibrated using DPPH. The spectra for the Co(II) samples were collected using the following instrument settings: for the ESP spectrometer, attenuation = 25 dB, microwave power = 0.63 mW, frequency = 9.21 GHz, sweep width = 4900 G, modulation amplitude = 5.02 Gpp, gain = 5.00×10^{-3}, conversion time = 40.96 ms, time constant = 1.28 ms, and resolution = 1024 points. Similar settings were used for the EMX spectrometer with the following exceptions: frequency = 9.30 GHz and conversion time = 164 ms. The spectra presented are the average of four scans. A copper standard spectrum was collected for each sample immediately after the sample EPR spectrum had been collected. Spin concentration of the EPR spectra for the Co polymer was determined by numerical integration of the unsaturated EPR spectra and compared with a Cu(II) standard (vide supra). Details of this procedure have been reported.[16]

The EPR spectra of the polymers were fit with the aid of the graphing program Kaliedagraph. The fits used the EPR spectra of P-**1**[Co^{II}] and P-**1**[Co^{II}(py)] as references. These two polymers have immobilized four- and five-coordinate Co(II) complexes, respectively. Their EPR spectra, along with that of P-**1**·**py**[Co^{II}], were spin-density quantified and normalized prior to simulation. An iterative method was used to simulate spectra. Ratios of the reference spectra were added and overlaid with the collected spectrum of P-**1**·**py**[Co^{II}] to achieve a best fit. The estimated errors in the simulated spectra are ∼10%.

Results and Discussion

Design Considerations. The immobilized metal sites have been designed such that the Co(II) ions are five-coordinate with a square-pyramidal coordination geometry.[17] This geometric requirement is necessary for Co(II) complexes to obtain the correct electronic configuration for O_2 binding: the energy of the d_{z^2} orbital needs to be raised above that of the d_{xy} orbital to give a $(d_{xz})^2(d_{yz})^2(d_{xy})^2(d_{z^2})^1$ configuration.[18] In contrast, square-planar Co(II) complexes are significantly less reactive toward O_2. This is illustrated in Scheme 1 for the solution binding properties [Co^{II}(salen)] (salen, bis(2-hydroxybenzaldehyde)-ethylenediimine).[19] Note that the four-coordinate Co^{II}(salen) complex weakly binds pyridine under anaerobic conditions but in the presence of dioxygen readily forms the tertiary Co(salen)-(py)(O_2) complex.

The approach shown schematically in Figure 1 was used to synthesize materials with immobilized sites having the correct arrangement of ligands to support square-pyramidal stereochemistry. A substitution-inert metal complex is the template that will determine the structure of the immobilized sites. We

Scheme 1[a]

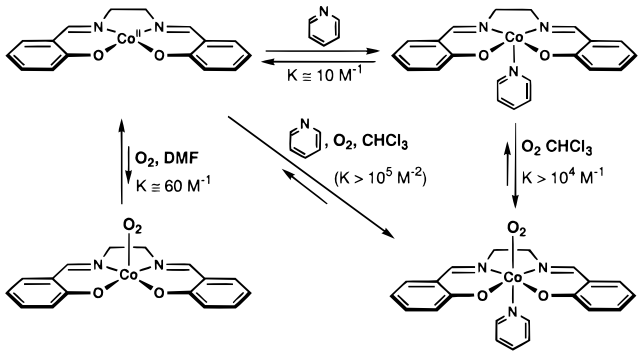

[a] Taken from ref 19.

reasoned that the use of an inert metal complex as a template would lead to materials whose immobilized sites would have similar architectures. Three covalent bonds (three-point immobilization) link the template to a highly cross-linked, porous organic host, two of which are in the equatorial plane and one that is positioned axially. The remaining coordinate site on the template is occupied by a nonpolymerizable ligand whose only connection to the polymer is through its bond to the metal ion. After copolymerization is completed, the metal ion and the nonpolymerizable ligand are chemically removed from the organic host. The immobilized sites thus contain endogenous ligands that are positioned for rebinding metal ions to form the desired square-pyramidal complexes. Moreover, the porous organic host sufficiently isolates the immobilized sites to prevent unwanted metal−metal interactions that lead to irreversible dioxygen binding, which is often found for similar complexes in solution.

Materials made by this design contain immobilized sites having endogenous donors that can form Co(II) complexes which are coordinatively unsaturated. The remaining coordination site is then able to bind guest molecules such as dioxygen. The void space around each metal center was created by the nonpolymerizable ligand that was removed from the immobilized site during demetalation. This method differs from our other published gas-binding systems that have immobilized sites containing tri- and tetradentate chelating ligands. Most of these earlier systems required the addition of external bases to form the needed coordination geometry to function as dioxygen binders.[9c] The placement of a pyridine ligand perpendicular to the equatorial coordination plane, as in this new design, replaces the need for binding of an external base. In addition, we can evaluate the extent to which the template effect can arrange ligands within the immobilized sites and compare the O_2-binding properties of the immobilized Co(II) centers to molecular analogues in solution.

[Co^{III}**1**(vpy)(dmap)]$^+$ was chosen as the template complex in this study because it has the requisite features for forming the immobilized metal sites (Scheme 2). These features include the following: (1) three appended vinyl groups that are needed for three-point immobilization, two from the bis[2-hydroxy-4-(4-vinylbenzyloxy)benzaldehyde]ethylenediimine (H_2**1**) and one from vpy; (2) an axially coordinated (dimethylamino)pyridine (dmap) ligand that is used to create void space for the binding of guest molecules; and (3) a complex that is diamagnetic and substitution-inert under the conditions of polymerization. Moreover, the rates of polymerization for vpy and styrene are similar enough to ensure that a majority of the immobilized sites have three-point immobilization.[20]

Synthesis. Scheme 2 outlines the synthesis of [Co^{III}**1**(vpy)-

(16) Krebs, J. K. Ph.D. Thesis, 1998, Kansas State University.

(17) (a) Jones, R. D.; Summerville, D. A.; Basolo, F. *Chem. Rev.* **1979**, *79*, 139−179 and references therein. (b) Niederhoffer, E. C.; Timmons, J. H.; Martell, A. E. *Chem. Rev.* **1984**, *84*, 137−203. (c) Norman, J. A.; Pez, G. P.; Roberts, D. A. In *Oxygen Complexes and Oxygen Activation by Transition Metal Metals*; Martell, A. E., Sawyer, D. T., Eds.; Plenum Press: New York, 1988; pp 107−127.

(18) (a) Carter, M. J.; Rillema, P. P.; Basolo, F. *J. Am. Chem. Soc.* **1974**, *96*, 392−400. (b) Meier, I. K.; Pearlstein, R. M.; Ramprasad, D.; Pez, G. P. *Inorg. Chem.* **1997**, *36*, 1707−1714.

(19) Cesarotti, M.; Gullotti, A.; Pasini, A.; Ugo, R. *J. Chem. Soc., Dalton Trans.* **1977**, 757−763.

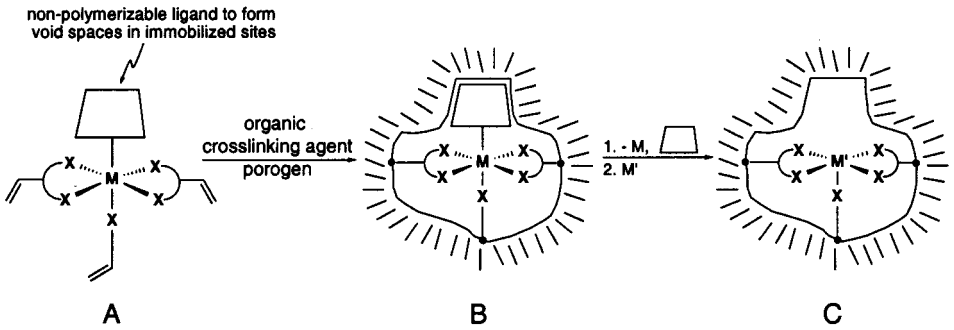

Figure 1. Schematic depiction of the template copolymerization method used for synthesizing coordinatively unsaturated metal sites immobilized in porous organic hosts: substitution-inert template complexes used to form the immobilized sites (A); immobilized sites after polymerization showing the spatial arrangement of ligands around the metal (B); and modified immobilized sites containing metal complexes with vacant coordination sites (C).

Scheme 2[a]

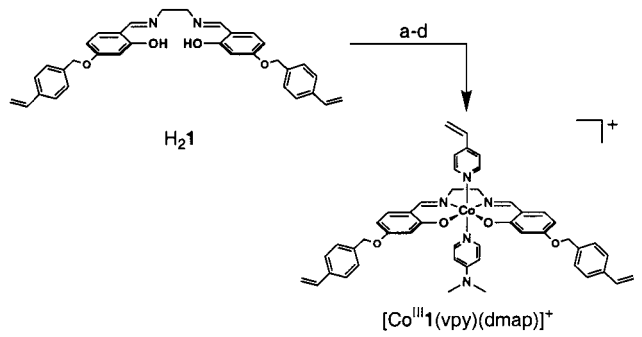

[a] Conditions: (a) $Co(OAc)_2$, DCE/MeOH, Ar; (b) dmap, DCE; (c) $[FeCp_2]FP_6$, CH_3CN; (d) 4-vinylpyridine, DCE.

(dmap)]PF_6. H_2**1** was treated with $Co^{II}(OAc)_2$ under an argon atmosphere to yield [Co^{II}**1**]. Without isolation, [Co**1**] was allowed to react with dmap to form [Co^{II}**1**(dmap)]. EPR spectroscopy confirms the formation of this complex. This five-coordinate Co(II) complex was oxidized with ferricenium and then treated with vpy to yield crude [Co^{III}**1**(vpy)(dmap)]PF_6. Purification was achieved by crystallization to afford the desired product in 78% yield. Analytical and spectroscopic measurements support that dmap and vpy are bonded to the Co(III) center in [Co^{III}**1**(vpy)(dmap)]$^+$. For example, the ^{1}H NMR spectrum of [Co^{III}**1**(vpy)(dmap)]$^+$ in $CDCl_3$ (Figure 2) is indicative of unsymmetrical axial coordination. In particular, the ethylene protons of **1** are diastereotopic, which was verified by the observed cross-peaks in the ^{1}H COSY spectrum of [Co^{III}**1**(vpy)(dmap)]$^+$ (inset in Figure 2).

[Co^{III}**1**(vpy)(dmap)]PF_6 was immobilized in a porous polymethacrylate matrix to form P-**1·py**[Co^{III}(dmap)] by the synthetic route shown in Scheme 3. This polymer was made by mixing 5 mol % of [Co^{III}**1**(vpy)(dmap)]PF_6, 94 mol % of EGDMA, and 1 mol % of AIBN in 3.32 mL of CH_3NO_2 and heating for 24 h at 60 °C. The template complex [Co^{III}**1**(vpy)-(dmap)]$^+$ is stable under these polymerization conditions as determined by NMR spectroscopy. The resulting dark red monolith was broken apart by grinding and subjected to continuous extraction with CH_3OH for 24 h to afford the red polymer P-**1·py**[Co^{III}(dmap)]. This polymer was dried under vacuum and sieved to a particle size of <125 μm. GC-MS analysis of the CH_3OH washings shows that neither dmap nor vpy were removed during extraction. Analytical and spectroscopic measurements indicate that the template complex remains

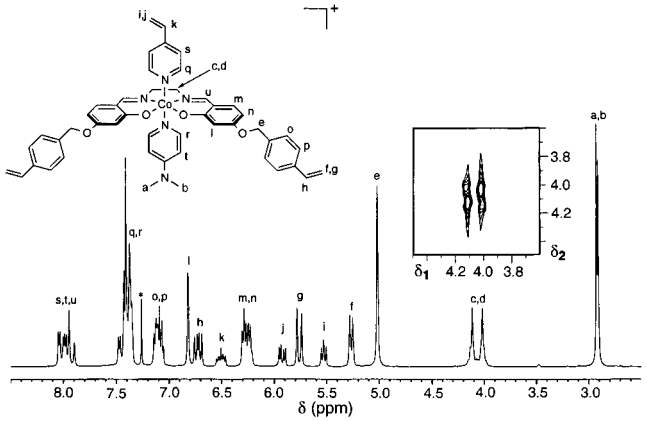

Figure 2. ^{1}H NMR (400 MHz) spectrum of the template complex [Co^{III}**1**(vpy)(dmap)]PF_6. The inset contains a portion of the ^{1}H NMR COSY spectrum of the complex, showing the cross-peaks for the diastereotopic protons (c and d) on the ethylene backbone of **1**.

intact after immobilization. The average amount of cobalt present in the polymer is 180 μmol of Co/g of polymer.

An efficient three-step procedure was employed to activate the immobilized metal sites in P-**1·py**[Co^{III}(dmap)] toward dioxygen (Scheme 3). The Co(III) centers in P-**1·py**[Co^{III}-(dmap)] were chemically reduced with a methanolic solution of $S_2O_4^{2-}$. Quantification of this reduction process by EPR spectroscopy shows that ~90% of the cobalt has been reduced to Co(II). Analysis by GC-MS of the CH_3OH used to wash the polymer after reduction reveals that only 10% of the dmap was removed at this step. P-**1·py**[Co^{II}(dmap)] was then treated with a methanolic solution of $(NMe_4)_2$EDTA to form the apo polymer P-**1·py**. This procedure extracted 85% of the Co(II) ions from the polymer and an additional 70% of the dmap ligand. P-**1·py** readily rebinds Co(II) to form P-**1·py**[Co^{II}], which has an average cobalt concentration of 170 μmol of Co/g of polymer. Loss of vpy from the polymer was not observed at any point during these chemical procedures, consistent with pyridine being covalently linked to the porous polymethacrylate host.

The chemical modification of P-**1·py**[Co^{III}(dmap)] to form P-**1·py**[Co^{II}] has only a small effect on the properties of the porous polymethacrylate host. The average surface area of P-**1·py**[Co^{II}] particles (270 m^2/g) is 15% higher than that found for the template polymer, P-**1·py**[Co^{III}(dmap)], particles (230 m^2/g). The pore diameters in the Co(II) polymers are also not affected by the chemical modifications at the immobilized sites. Average pore diameters are 22 Å, which remains constant for P-**1·py**[Co^{III}(dmap)], P-**1·py**, and P-**1·py**[Co^{II}]. The mesoporous character of P-**1·py**[Co^{III}(dmap)] and P-**1·py**[Co^{II}] is shown in the SEM images in Figure 3.

(20) *Polymer Handbook*, 4th ed.; Bramdrup, E., Immergut, E., Grulke, E., Eds.; John Wiley and Sons: New York, 1990; p 290.

Scheme 3[a]

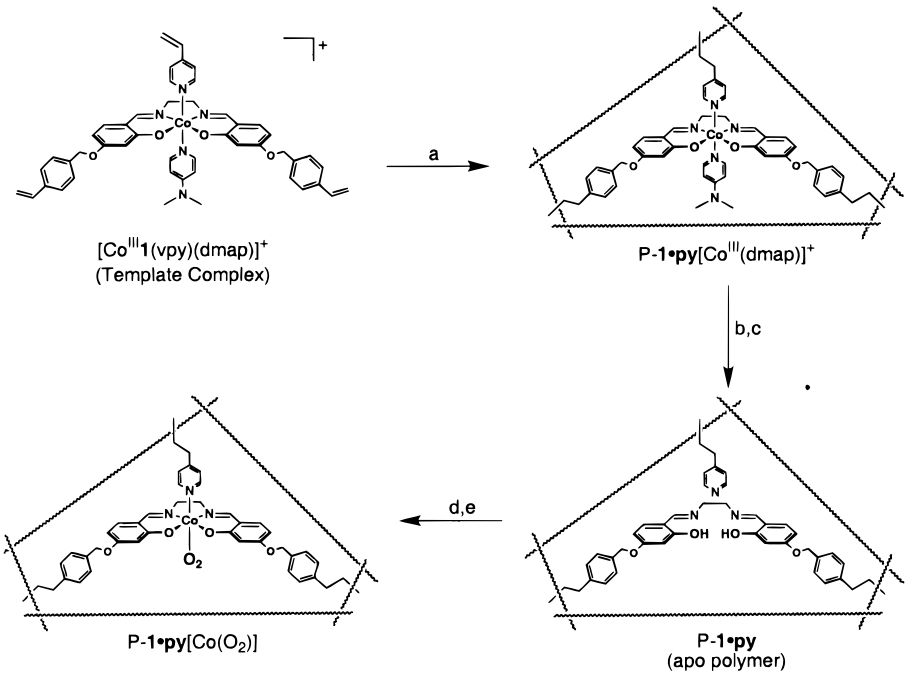

[a] Conditions: (a) EGDMA, AlBN, CH_3NO_2, Ar, 60 °C, 24 h; (b) $Na_2S_2O_4$, MeOh, Ar, 2 h; (c) $(NMe_4)_2EDTA$, MeOH, Ar, 24 h; (d) $Co(OAc)_2$, MeOH, Ar, 6 h; (e) O_2, CH_3NO_2.

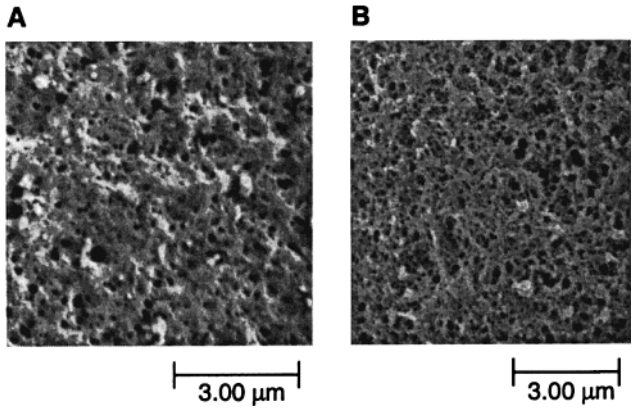

Figure 3. SEM images showing the porosity of P-**1**·**py**[Co^{III}(dmap)] (A) and P-**1**·**py**[Co^{II}] (B).

EPR Spectroscopy of P-1·py[Co^{II}]. EPR spectroscopy has been used in molecular systems to probe the structure of low-spin Co(II) complexes.[17,21] We have shown previously that this technique can also differentiate various coordination geometries around Co^{II}(salen) complexes immobilized in porous organic hosts.[9c] For example, P-**1**[Co^{II}] and P-**1**[Co^{II}(py)], which have square-planar and square-pyramidal immobilized sites in porous polymethacrylate hosts (Chart 1), give distinctly different X-band EPR spectra at 77 K. As shown in Figure 4a, an axial EPR spectrum is obtained for a suspension of P-**1**[Co^{II}] in CH_3NO_2 with g-values at 3.83 and 1.98. For P-**1**[Co^{II}(py)] suspended in CH_3NO_2, a rhombic spectrum is produced, which is consistent with a square-pyramidal Co(II) complex: $g_1 = 2.45$; $g_2 = 2.25$; $g_3 = 2.02$; $A_3 = 96$ G; $a_3^N = 16$ G. Both these EPR spectra originate from ground $\pm^1/_2$ doublets of the low-spin Co(II) centers.[21,22] A more complicated X-band EPR spectrum is observed for a suspension of P-**1**·**py**[Co^{II}] in CH_3NO_2 (Figure 4b). Simulation of the spectrum reveals that 60% of the immobilized sites in P-**1**·**py**[Co^{II}] have square-pyramidal Co(II) centers and 40% have square-planar centers. The ratio of five- to four-coordinate sites is affected by the solvent in which the polymer is suspended. In $CH_3CH(NO_2)CH_3$ and $C_6H_5NO_2$, approximately 45% of the immobilized sites contain five-coordinate Co(II) centers. The percentage of five-coordinate sites drops to 30% when the polymer is suspended in diethyl ether and cyclohexane (Figure 4c).

Chart 1

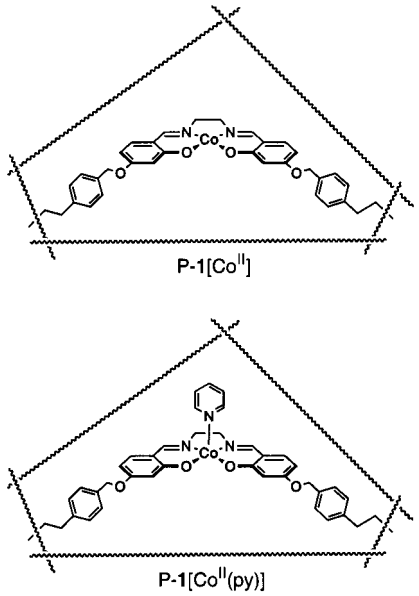

These results are consistent with an equilibrium of four- and five-coordinate Co(II) complexes in the immobilized sites of

(21) (a) Walker, F. A. *J. Am. Chem. Soc*. **1970**, *92*, 4235−4244. (b) Hoffman, B. M.; Diemente, D. L.; Basolo, F. *J. Am. Chem. Soc*. **1970**, *92*, 61−65. (c) Walker, F. A. *J. Magn. Reson.* **1974**, *15*, 201−218. (d) Walker, F. A.; Bowen, J. *J. Am. Chem. Soc*. **1985**, *107*, 7632−7635. (e) Bowen, J. H.; Shokhirev, N. V.; Raitsimring, A. M.; Buttlaire, D. H.; Walker, F. A. *J. Am. Chem. Soc*. **1997**, *101*, 683−691.

(22) Drago, R. *Physical Methods in Chemistry*; Saunders: Philadelphia, 1977; Chapter 13.

Chart 2

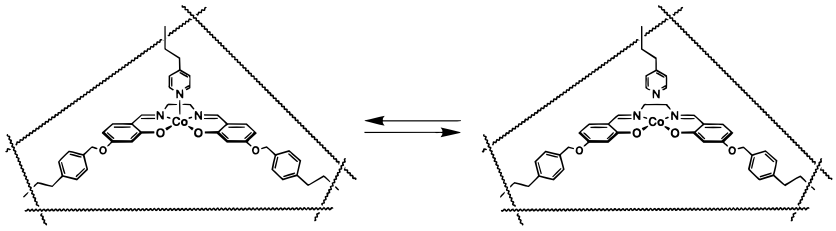

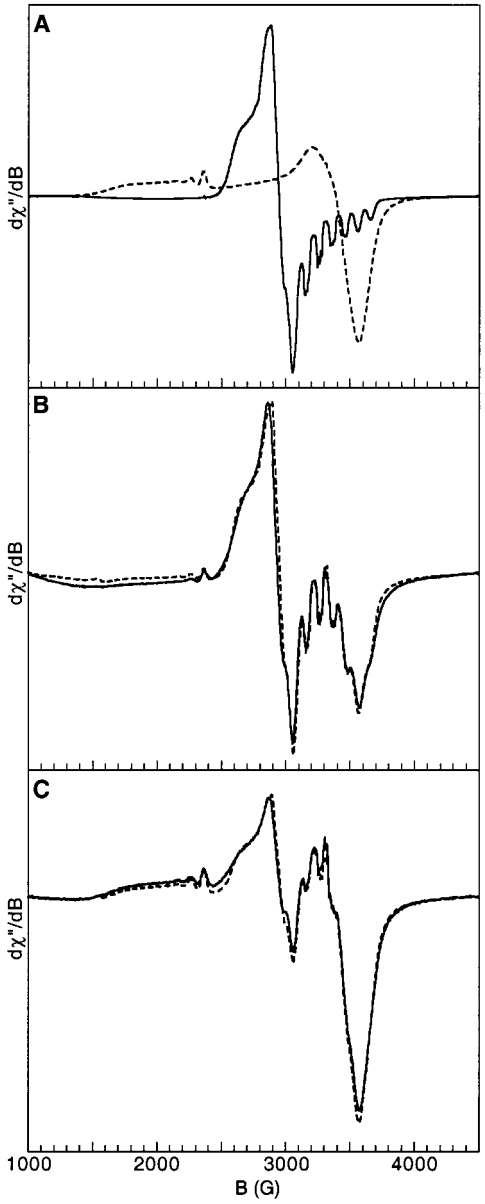

Figure 4. X-band EPR spectra measured at 77 K for P-**1**[Co^{II}] (—) and P-**1**[Co^{II}(py)] (- - -) suspended in CH_3NO_2 (A), and P-**1·py**[Co^{II}] suspended in CH_3NO_2 (B) and cyclohexane (C). The spectral fits are indicated by broken lines in panels B and C.

P-**1·py**[Co^{II}] (Chart 2). Similar equilibria have been reported for Co(II) complexes in solution (Scheme 1).[19,23] The observation of an equilibrium of sites in P-**1·py**[Co^{II}] indicates that, while the endogenous pyridine and salen ligands are correctly positioned within the site, they may not be rigidly held (i.e., preorganized).[24] A possible cause for this intra-site flexibility is the three-point immobilization used to produce the cobalt sites. The strylyoxy and vinyl linker groups that connect the endogenous ligands to the polymethacrylate host are inherently flexible. The binding of the axial pyridine ligand to the immobilized Co^{II}**1** centers should be weak based on molecular systems studied in solution. Thus, a small degree of conformational flexibility between the pyridine and salen ligands within the sites will give rise to a distribution of four- and five-coordinate sites.[25] The highest degree of five-coordinate sites occurs when P-**1·py**[Co^{II}] is suspended in CH_3NO_2, the solvent used during polymerization. The swelling of the polymer in different solvents does not account for this observation. The swelling ratio of P-**1·py**[Co^{II}] in CH_3NO_2 and $C_6H_5NO_2$ are not significantly different but the percentages of five-coordinate sites in these solvents differ by a factor of 1.5. We suggest that a "solvent memory" effect influences the formation of the immobilized sites which, in turn, affects the Co(II) coordination geometry. During the copolymerization process it is reasonable to assume that the template complex is solvated. The actual template is thus a combination of a Co(III) complex and a number of CH_3NO_2 molecules. When P-**1·py**[Co^{II}] is suspended in CH_3NO_2, the immobilized Co(II) sites can accommodate the CH_3NO_2 molecules and the greatest percentage of five-coordinates sites is observed. When other solvents not present at polymerization are used to suspend the polymer, they can interfere with the binding of the pyridine ligand which leads to a lower percentage of 5-coordinate Co(II) sites. This solvent memory effect has been reported for other materials made by template copolymerization methods.[26] In these other systems, the highest degree of rebinding of a chiral template occurs in the solvent in which the polymer was synthesized. The intra-site binding observed in P-**1·py**[Co^{II}] agrees with these results and illustrates the importance of the synthetic conditions in forming the immobilized sites.

The above explanation for the distribution of four- and five-coordinate immobilized Co(II) complexes in P-**1·py**[Co^{II}] does not consider heterogeneous architectures where some sites are without the templated pyridine ligand. This possibility was ruled out because (i) free 4-vinylpyridine was not detected at any point in the synthesis of P-**1·py**[Co^{II}], (ii) nitrogen analysis of P-**1·py**[Co^{II}] supports the presence of pyridine in the polymer; and (iii) nearly all the immobilized Co(II) sites in P-**1·py**[Co(II)] reversibly bind dioxygen (vide infra).

Dioxygen Binding to P-1·py[Co^{II}]. Exposure of a suspension of P-**1·py**[Co(II)] to dioxygen in CH_3NO_2 for 2 min affords complete conversion to the Co−O_2 polymer, P-**1·py**[Co−O_2]. A well-resolved anisotropic EPR signal is observed for P-**1·py**[Co−O_2], with EPR parameters of $g_1 = 2.08$; $g_2 = 1.99$; $g_3 = 1.96$; $A_1 = 19$ G; $A_3 = 15$ G (Figure 5a). This signal is consistent with dioxygen binding directly to the immobilized Co(II) centers.[20,27] Comparable spectra have been reported for

(23) Walker, F. A. *J. Am. Chem. Soc.* **1973**, *95*, 1150−1153.
(24) (a) Cram, D. J. *Angew. Chem., Int. Ed. Engl.* **1988**, *27*, 1009−1020. (b) Sanders, J. K. M. *Chem. Eur. J.* **1998**, *4*, 1378−1383.
(25) For a study on the effects of linker groups in templated copolymers see: Dhal, P. K.; Arnold, F. H. *New J. Chem.* **1996**, *20*, 695−698.
(26) Allender, C. J.; Heard, C. M.; Brian, K. R. *Chirality* **1997**, *9*, 238−242 and references therein.

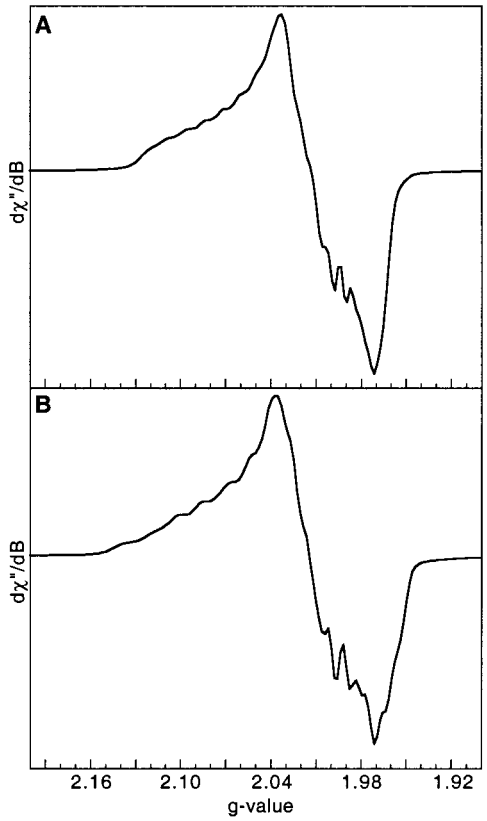

Figure 5. X-band EPR spectra measured at 77 K for CH_3NO_2 (A) and cyclohexane (B) suspensions of P-**1**·**py**[Co−O_2].

dioxygen adducts of molecular Co(II) complexes.[17,21,28] The spin concentration of this signal is ∼160 μm/g of polymer, showing that approximately 90% of the immobilized cobalt sites are binding dioxygen. This value is larger than what we have reported previously for other immobilized Co(II) complexes.[9c] In these other systems, the highest percentage of dioxygen binding to cobalt sites was 70%. Moreover, the percentage of cobalt sites that stabilize Co−O_2 adducts in P-**1**·**py**[Co−O_2] is significantly higher than those reported for similar complexes immobilized in zeolite cages.[29] For example, only 1% of the cobalt sites are oxygenated in zeolite NaY containing immobilized Co^{II}(salen)(py) complexes.[29g]

The formation of the P-**1**·**py**[Co−O_2] is independent of solvent used in suspending the polymer. When suspensions of P-**1**·**py**[Co^{II}] in other solvents are treated with dioxygen, nearly identical EPR spectra for P-**1**·**py**[Co−O_2] are obtained to that observed in CH_3NO_2. Figure 5b illustrates an example of this spectral similarity for P-**1**·**py**[Co−O_2] suspended in cyclohexane (EPR parameters: $g_1 = 2.08$; $g_2 = 2.00$; $g_3 = 1.96$; $A_1 = 26$ G; $A_3 = 14$ G). The spectrum obtained in cyclohexane is slightly broader (∼50 G) than the one measured in CH_3NO_2 (Figure 5a). The well-resolved signals observed for these suspensions suggest that the immobilized Co−O_2 complexes have similar structures, with little heterogeneity at the metal centers.

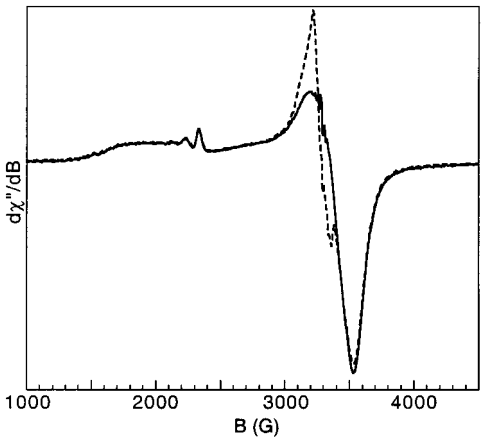

Figure 6. X-band EPR spectra measured at 77 K for a cyclohexane suspension of P-**1**[Co^{II}] under an atmosphere of Ar (— and O_2 (- - -).

Furthermore, the spectra of P-**1**·**py**[Co−O_2] do not contain signals that can be ascribed to the four-coordinate Co(II) complexes. The lack of a four-coordinate signal implies that the endogenous pyridine ligands in the immobilized sites are positioned within bonding distance of the cobalt centers. This positioning is required to form the immobilized Co**1**(py)(O_2) complexes that yield the observed EPR spectra (vide supra). To support this idea, we have examined the dioxygen binding properties of P-**1**[Co^{II}], a material containing purely four-coordinate Co(II) complexes immobilized within the same porous polymethacrylate host. P-**1**[Co^{II}] has limited dioxygen binding with <5% of the sites forming the Co−O_2 adducts. This lack of O_2 binding is illustrated in Figure 6 for a suspension of P-**1**[Co^{II}] in cyclohexane. Note that lack of dioxygen binding to the four-coordinate Co(II) sites in P-**1**[Co^{II}] is in agreement with observations for monomeric Co(II) complexes in solution (Scheme 1).

P-**1**·**py**[Co^{II}] reversibly binds dioxygen at room temperature. The reversibility was monitored by EPR spectroscopy and results for suspensions of P-**1**·**py**[Co^{II}] in CH_3NO_2 and cyclohexane are shown in Figure 7. Removal of dioxygen from P-**1**·**py**[Co−O_2] is accomplished by flushing the system with N_2 for 3 min. Rebinding of O_2 to P-**1**·**py**[Co^{II}] produces identical EPR spectra to that obtained initially for P-**1**·**py**[Co−O_2]. Spin concentration studies of the spectra associated with P-**1**·**py**[Co−O_2] show no decomposition of the cobalt binding sites during oxygenation.

The dioxygen binding results of P-**1**·**py**[Co^{II}] contrast those obtained with the molecular species, Co**1**(py).[9c] For complex dissolved in a 1:1 dichloromethane−toluene mixture, <10% of the Co−O_2 complex are stable and no reversible binding is observed at room temperature. This control experiment illustrates the importance of the porous organic host in isolating the Co−O_2 sites. The isolation of the Co−O_2 sites in P-**1**·**py**[Co−O_2] prevents unwanted metal−metal interactions that limit reversibility. These types of intermolecular interactions often impede the functional capabilities of soluble metal−dioxygen complexes.

Summary and Conclusions. The results obtained from this study demonstrate that template copolymerization of substitution inert metal complexes is an effective way of designing immobilized metal ion sites in polymeric hosts. This method allows the control of the geometry around coordinatively unsaturated metal ions immobilized in porous organic hosts as was shown for P-**1**·**py**[Co^{II}]. Few studies on materials made by template copolymerization methods have directly probed the structure of the immobilized sites.[11] The structural properties of the sites are often inferred from data obtained through batch rebinding

(27) Tovrog, B. S.; Kitko, D. J.; Drago, R. S. *J. Am. Chem. Soc.* **1976**, *98*, 5144−5153.
(28) Getz, D.; Melemud, E.; Silver, B. C.; Dori, Z. *J. Am. Chem. Soc.* **1975**, *97*, 3846−3847.
(29) (a) Howe, R. F.; Lunsford, J. H. *J. Phy. Chem.* **1975**, *75*, 1836−1842. (b) Herron, N. *Inorg. Chem.* **1986**, *25*, 4714−47. (c) Howe, R. F.; Lunsford, J. H. *J. Am. Chem. Soc.* **1994**, *116*, 4746−4752. (d) Dutta, P. K.; Bowers, C. *Langmuir* **1991**, *7*, 937−940. (e) Drago, R. S.; Gaul, J.; Zombeck, A.; Straub, D. K. *J. Am. Chem. Soc.* **1980**, *102*, 1033−1038. (f) Taylor, R. J.; Drago, R. S.; Hage, J. P. *Inorg. Chem.* **1992**, *31*, 253−258. (g) De Vos, D. E.; Feijen, E. J. P.; Schoonheydt, R. A.; Jacobs, P. A. *J. Am. Chem. Soc.* **1994**, *116*, 4746−4752.

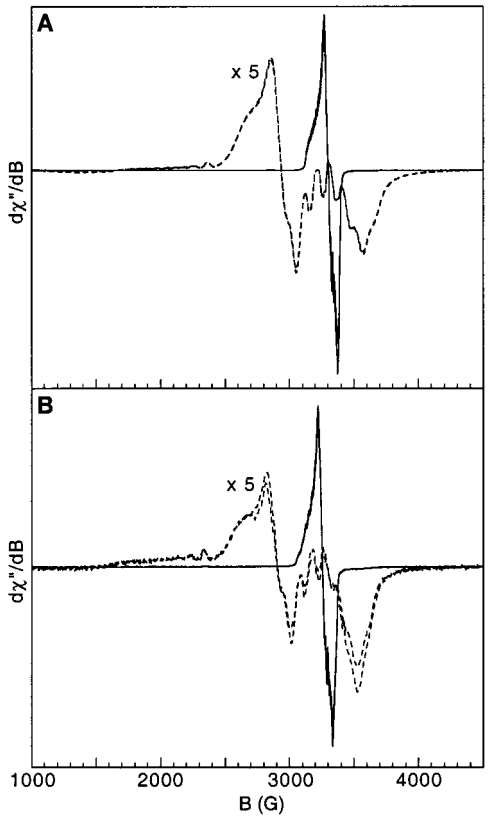

Figure 7. X-band EPR spectra measured at 77 K for CH_3NO_2 (A) and cyclohexane (B) suspensions of P-**1·py**[Co^{II}] (- - -) showing reversible dioxygen binding to form P-**1·py**[$Co-O_2$] (—). Two cycles are presented.

studies or mechanistic considerations. Using EPR spectroscopy, we have successfully characterized the coordination geometry of the Co(II) complexes within the immobilized sites. In P-**1·py**[Co^{II}], the weak binding of pyridine ligands to paramagnetic Co(II) complexes is a sensitive probe for examining the coordination geometry of the immobilized complexes. The presence of four- and five-coordinate Co(II) complexes in P-**1·py**[Co^{II}] is attributed to an equilibrium established in the immobilized sites. A similar equilibrium is observed in solution for the binding of pyridine to Co(II)salen. This type of structural equilibrium is consistent with the pyridine ligand in each immobilized site being in the correct position to bond axially to the labile Co(II) centers. Additional support for this site structure is given by the complete conversion of P-**1·py**[Co^{II}] to P-**1·py**[$Co-O_2$]. Immobilized Co(II)salen complexes require an additional axial ligand to achieve this high of a degree of dioxygen binding. This can be attained by the binding of the endogenous pyridine ligands to form six-coordinate Co(salen)(py)(O_2) complexes within the immobilized sites. The low percentage of $Co-O_2$ sites in P-**1**[Co^{II}], which has immobilized sites containing purely four-coordinate Co(II) complexes, illustrates the need for incorporating an additional axial pyridine ligand to achieve reversible O_2 binding.

Polymers made by template copolymerization methods often have lower than expected selectivity for the rebinding of their template molecules.[7] This is ascribed to structural heterogeneity in the immobilized sites. Spatial misplacement of the functional groups within the immobilized sites is one possible cause for this heterogeneity.[30] Studies on the structure of immobilized Co(II) complexes in P-**1·py**[Co^{II}] indicate that the 4- and 5-coordinate complexes present within the sites result from the conformational flexibility of ligands, as opposed to misplacement of the ligands. This flexibility is attributed to the nonrigidity and low number of vinyl and strylyoxy linkers used to connect the ligands to the polymer host. It is likely that similar types of conformational flexibility are present in other polymers made by this method. In fact, the majority of templated copolymers use only one linker to connect each functional group to the rigid polymer host. This results in rotamers being present in the immobilized sites that could contribute to the nonselective binding of analytes. Note that conformational flexibility of ligands in the immobilized sites of P-**1·py**[Co^{II}] does not hinder its functional properties, as shown by 90% of the sites being able to reversibly bind dioxygen. In fact, conformational flexibility at the immobilized metal sites, as observed in P-**1·py**[Co^{II}], can be advantageous if applied correctly, such as in catalyst development.[7c,31]

The superior dioxygen binding ability of P-**1·py**[Co^{II}] results from the architecture of the immobilized cobalt sites and the site isolation capability of the porous polymethacrylate host. This combination of structural properties is essential for developing functional materials that utilize metal complexes. This is especially true for those systems involving the reversible binding and/or activation of dioxygen. Other methods have been reported for the synthesis of O_2 binding materials that include the attachment of complexes through one ligand group to a preformed cross-linked polymeric support[32] and encapsulation of cobalt or iron complexes inside the cages of zeolite[29] or dendrimers.[33] While some promising results have been obtained, several of these systems do not sufficiently isolate the metal sites from each other, and thus have low O_2-binding capacities.[34] The synthetic methodology described in this work differs fundamentally from these other approaches. The assembly of polymers from monomeric, substitutionally inert metal complexes and organic cross-linking agents provides a level of molecular control that is often difficult to achieve in solid-state materials. The immobilized cobalt sites in P-**1·py**[Co^{II}] retain properties of their molecular components in solution as is seen in the weak intra-cavity binding of pyridine. Moreover, a high percentage of Co(II) sites in P-**1·py**[Co^{II}] reversibly bind dioxygen, which is a significant improvement over related molecular systems that lack a protective porous host.

Acknowledgment. We thank Drs. John Krebs and Vivek Joshi for their invaluable advice during the course of this study.

(30) Heterogeneous site structure is observed with templates formed from either covalent or noncovalent interactions; however, heterogeneity is more prevalent in systems that use noncovalent templates.

(31) Koshland, D. E., Jr. *Angew. Chem., Int. Ed. Engl.* **1993**, *33*, 2375−2378. (b) Gerstein, M.; Lesk, A. M.; Chothia, C. *Biochemistry* **1994**, *33*, 6739−6749.

(32) (a) Wang, J. H. *Acc. Chem. Res.* **1970**, *3*, 90−97. (b) Collman, J. P.; Reed, C. A. *J. Am. Chem. Soc.* **1973**, *95*, 2048−2049. (c) Leal, O.; Anderson, D. L.; Bowman, R. G.; Basolo, F.; Burwell, R. L., Jr. *J. Am. Chem. Soc.* **1975**, *97*, 5152. (d) Tsuchida, E.; Nishide, N. *Adv. Polym. Sci.* **1977**, *24*, 1−87. (e) Wohrle, D.; Bohlen, H.; Aringer, C.; Pohl, D. *Makromol. Chem.* **1984**, *185*, 669−685.

(33) Aida, T.; Jiang, D.-L. *Chem. Commun.* **1996**, 1523−1524. (b) Collman, J. P.; Fu, L.; Zingg, A.; Diederich, F. *Chem. Commun.* **1997**, *2*, 193−194.

(34) Molecular systems that bind dioxygen have also been reported, most notably are complexes of sterically encumbered porphyrins,[35a−e] imine bases,[35f] and polycyano ligands.[19b,35g] (a) Collman, J. P. *Acc. Chem. Res.* **1977**, *10*, 265−272. (b) Momenteau, M.; Reed, C. A. *Chem. Rev.* **1994**, *94*, 659−698. (c) Collman, J. P.; Zhang, X.; Herrmann, P. C.; Uffelman, E. S.; Boitrel, B.; Atraumanis, A.; Brauman, J. I. *J. Am. Chem. Soc.* **1994**, *116*, 2981. (d) Collman, J. P. Zhang, X.; Wong, K.; Brauman, J. I. *J. Am. Chem. Soc.* **1994**, *116*, 6245−6251. (e) Collman, J. P.; Herrmann, P. C.; Boitrel, B.; Zhang, X.; Eberspacher, T. A.; Fu, L. *J. Am. Chem. Soc.* **1994**, *116*, 9783−9784. (f) Busch, D. H.; Alcock, N. W. *Chem. Rev.* **1994**, *94*, 585−623. (g) Ramprasad, D.; Pez, G. P.; Toby, B. H.; Markley, T. J.; Pearlstein, R. M. *J. Am. Chem. Soc.* **1995**, *117*, 10694−10701.

We also thank Professors C. Loudon and B. Subramaniam for helpful discussions, Dr. B. Culter for help in obtaining the SEM images, and D. Bochniak for obtaining the surface area and pore diameter measurements. Financial support of this work was provided by ONR-DEPSCoR and the NIH. The Bruker EMX-EPR spectrometer was purchased with funds obtained from the ONR-DURIP program.

JA0014739